MONITORING LAND SUBSIDENCE IN ULAANBAATAR, MONGOLIA BASED ON PS- INSAR TECHNOLOGY

Yuxin Xie[1], Hasi Bagan*[1], Luwen Tan[1], Yune La[2], Tonghua Wu[3], Bayarsaikhan Uudus[4] and Qinxue Wang[5]

[1]School of Environmental and Geographical Sciences, Shanghai Normal University, No.100, Guilin Road, Xuhui District, Shanghai 200234, China,
Email: 1000527330@smail.shnu.edu.cn; hasibagan@staff.shnu.edu.cn; 1000495878@smail.shnu.edu.cn
[2]Cryosphere Research Station on the Qinghai-Tibetan Plateau, State Key Laboratory of Cryospheric Science, Northwest Institute of Eco-Environment and Resource, Chinese Academy of Sciences, Lanzhou 730000, China,
Email: layune20@mails.ucas.ac.cn
[3]Cryosphere Research Station on the Qinghai-Tibetan Plateau, State Key Laboratory of Cryospheric Science, Northwest Institute of Eco-Environment and Resource, Chinese Academy of Sciences,Lanzhou 730000, China; Southern Marine Science and Engineering Guangdong Laboratory, Guangzhou 511458, China,
Email: thuawu@lzb.ac.cn
[4]National University of Mongolia, Ulaanbaatar 210646, Mongolia,
Email: bayaraa@num.edu.mn
[5]National Institute for Environmental Studies, Tsukuba, Ibaraki 305-8506, Japan,
Email: wangqx@nies.go.ip

KEY WORDS: Land Deformation, Urbanization, Sentinel-1, Permanent Scatterer, Uplift

ABSTRACT: With the global urbanization, land subsidence has become one of the major disasters facing urban development. In recent decades, more than 50% of the country's population lives in Ulaanbaatar, Mongolia. The continued urban expansion and severe groundwater exploitation may lead to ground subsidence in Ulaanbaatar. Therefore, monitoring the ground subsidence is important for disaster prevention in Ulaanbaatar. Traditional monitoring based on GPS and geometrical leveling can obtain the subsidence of ground points. However, these methods are time consuming and measure not large area but a single point. With the development of differential interference radar (D-InSAR) technology, time-series InSAR technology provides accurate and low-cost technical approach for monitoring land subsidence over a large area. The time-series InSAR technology based on Permanent Scatterer (PS) (PS-InSAR) utilizes permanent scatterers that are relatively stable in time series. By analyzing the phase changes of these permanent scatterers in time series, the influence of atmosphere can be eliminated. So it can invert the high-precision land subsidence information of the study area, and perform the land subsidence monitoring at millimeter-level. In this study, we used the long-term Sentinel-1 satellite data from 2017 to 2020 to generate the high-precision land subsidence in Ulaanbaatar based on PS-InSAR technology. The results showed that: (1) for the study area, the PS-InSAR method is superior to the SBAS-InSAR method. (2) Most areas have light uplift and some areas have subsidence. The average displacement rate and the the standard deviation were 0.17 and 1.01 mm/year. And the land deformation is in a stable condition overall during the recent years. (3) The ground deformation is mainly stable in the central area of the city, while the light uplift is mainly in the edge. And land subsidence is more obvious near roads and rivers.

1. INTRODUCTION

With the global urbanization, land subsidence has become one of the major disasters facing urban development(Pradhan et al., 2014). In particularly, densely populated cities, which contain many buildings, are often vulnerable to subsidence. This subsidence may cause economic damage(Raspini et al., 2014) to the city and

may give rise to other disasters. Some disasters are listed below. Firstly, it may cause sinking and damage to the building such as scrapping of Tangshan Gymnasium Project due to the land subsidence. Secondly, it may lead to the damage of municipal facilities, such as hazards to natural gas pipelines(Qruji et al., 2022). Thirdly, land subsidence could affect the flooding protection in urban city such as Tianjin, Suzhou, Changzhou, etc. Moreover, land subsidence causes unevenness of roads, adding many unsafe factors to road and railroad transportation. Therefore, monitoring the ground subsidence is extremely important for urban development and disaster prevention.

In recent years, land subsidence monitoring methods have been divided into two main categories: one is traditional monitoring based on GPS and geometrical leveling(Jian et al., 2011), and the other is interferometric synthetic aperture radar (InSAR) techniques(Amelung et al., 1999). Among them, traditional monitoring can obtain the subsidence of ground points. However, these methods are time consuming and measure not large area but a single point. While time-series InSAR techniques(Cianflflone et al., 2015), such as permanent scatterer synthetic aperture radar interferometry (PS)(PS-InSAR) and small baseline subset (SBAS) techniques can provide higher spatial and temporal resolution, large area ground subsidence results. In the past years, many scholars have conducted related studies, such as Fikri S(Fikri et al., 2021), Aguiar Pedro(Aguiar et al., 2021), Lyu Mingyuan(Lyu et al., 2020), Zhang Xin(Zhang et al., 2022), Yuan Mingze(Mingze et al., 2021), Milillo(Milillo et al., 2019), Xiong Siting(Xiong et al., 2021) and etc. Among them, Milillo et al. applied PS-InSAR analysis to the Envisat data spanning 2003–2011, the COSMO-SkyMed and the Sentinel-1A/B spanning 2009–2018(Milillo et al., 2019). Xiong Siting et al. applied PS-InSAR analysis to derived Displacements of the Hong Kong–Zhuhai–Macao Bridge (HZMB) from Sentinel-1A Observations(Xiong et al., 2021).

In this study, Sentinel-1 was processed using PS-InSAR to identify the land subsidence of Ulbaanbaatar. Moreover, we also generated the mean velocity(mm/year) maps of the final geocoded displacements and analyzed the possible reasons in the context of other information. The observed results can provide useful information for identifying and understanding the behavior of the land subsidence phenomenon, which plays an important role in urban development and disaster prevention.

2. STUDY AREA

Ulaanbaatar, the capital of Mongolia, is the economic, political, commercial and cultural centre of the country. It is located in the middle of the Mongolian plateau(47°55′12N， 106°55′12E), and is surrounded by mountains to north and south, with an altitude of 1350 meters. The city centre is laid out along the Tula River in a narrow east-west direction. Located inland, it has a typical continental climate, with a relatively dry climate, annual precipitation of 280 mm and an average annual temperature of -1.9 degrees Celsius. Ulaanbaatar covers an area of 470,700 hectares, which is equivalent to 3% of the country's land area, with only 5.5% of the urban area, most of which is pastoral. However, Mongolia continues to experience high levels of rural to urban migration(Hamiduddin et al., 2021). In particular, Ulaanbaatar, where more than 50% of the country's population lives, is home to most of the country's factories and businesses. In this study, the central city of Ulaanbaatar is selected as the study area, as shown in Figure 1.

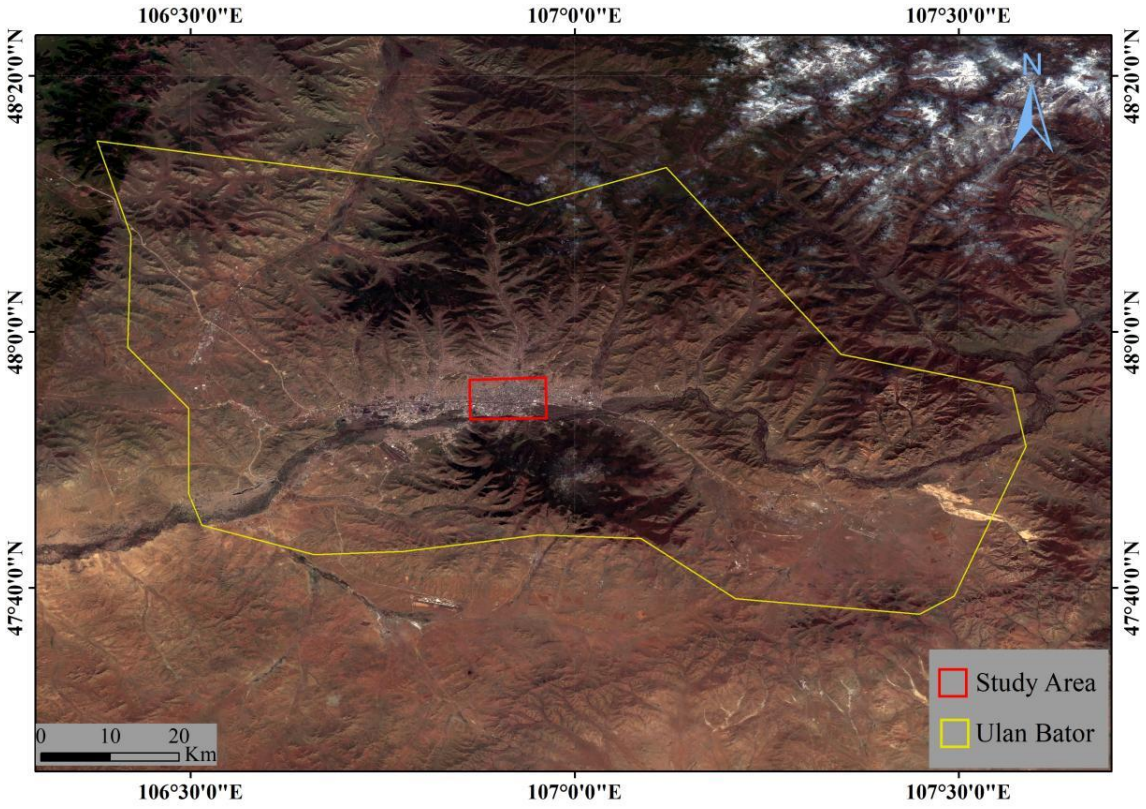

Figure 1.The map of the study area, Ulaanbaatar, Mongolia

3. DATA AND METHOD

3.1. Data

In this study, the SAR data collected by the Sentinel-1 satellite were used to monitor the land subsidence of Ulaanbaatar. A total of 24 single look complex (SLC) scenes were provided by the Alaska Satellite Facility(ASF). The SLC data is the first level product that has been processed. The phase and amplitude information can be obtained. The phase information is a function of time, and the distance measurement can be realized based on the phase information and velocity, which can be used for distance measurement and deformation observation. The spatial resolution is 15 meters and VV polarization method were selected.

3.2. Method

With the development of differential interference radar (D-InSAR) technology, time-series InSAR technology provides accurate and low-cost technical approach for monitoring land subsidence over a large area. Therefore, this study adopted the technique of time-series InSAR to monitor the ground deformation. Currently, the main time-series InSAR methods are PS-InSAR and SBAS-InSAR. PS-InSAR technology utilizes permanent scatterers that are relatively stable in time series to analyse the phase changes over time series. This can achieve millimetre-level land deformation monitoring and extrapolate the deformation rate over the period. The SBAS method utilizes distributed scatterers from all available SAR images with corresponding small baselines in order to reduce the spatial decorrelation and obtain the time-series displacements. PS-InSAR has a high sensitivity to slow displacement, with PS density points typically higher in areas of high reflectivity, such as urban areas, while SBAS performs better in non-urban vegetated areas and areas of high deformation rate(Yusupujiang et al., 2018). In this paper, using PS-InSAR technology to generate the high-precision land subsidence relied on the fact that the study area was the urban section of Ulaanbaatar. For SBAS-InSAR,

PS-InSAR is done by analyzing the timing phase information of the stable PS points, and therefore, has a higher inversion accuracy.

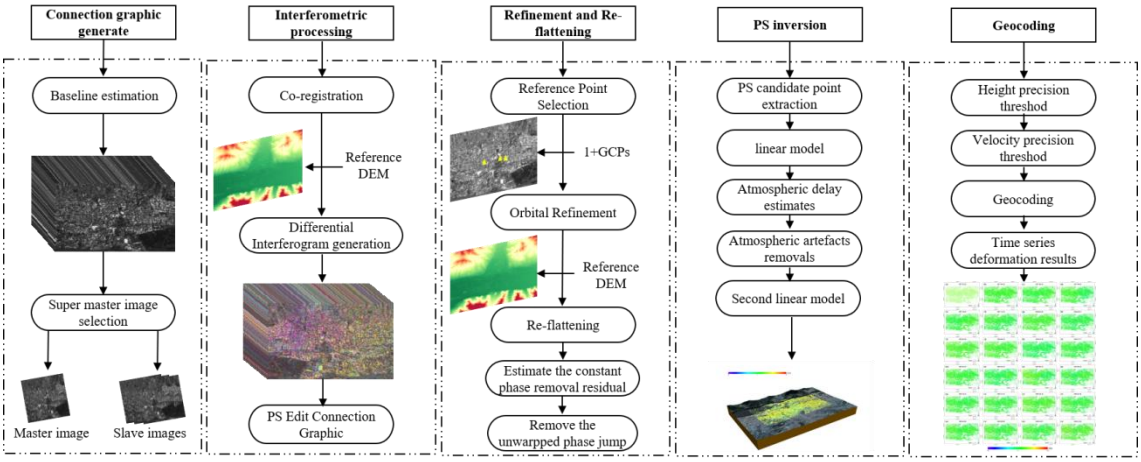

Figure 2 The processing flow of PS-InSAR

The Sentinel-1 data were processed using PS-InSAR technology. The SARscape®Modules (5.6.2) for ENVI (5.6.2) software suite (HARRIS Geospatial Solutions, Broomfifield, CO, USA) was employed to perform the interferometric analyses. We generated a total of 24 interferograms. The PS-InSARd processing flow chart is shown in Figure 2. We can see that the PS-InSAR process includes five main steps. The fist step is Connection graphic generation, including baseline estimation and super master image selection. As shown in Figure 3, the PS-InSAR pairs were generated with respect to the master image from 9 June 2020. In the second part—Interferometric processing, co-registration was processed to make all images geometrically consistent with the super master image which used DEM data as a reference. Then a series of interferograms are generated. The third step was Refinement and Re-flattening, including reference point selection, orbital refinement, re-flattening and etc. which can estimate and remove the residual constant phase and the unwrapped phase jump. The next step, PS inversion, which includes PS candidate point extraction and two inversions of deformation, could remove the atmospheric phase component and obtain the final deformation rate. It should be noted that linear inversion model was used twice in this process. The last step was Geocoding to output the reliable time-series deformation results. And this step included setting height and velocity precision threshold and geocoding.

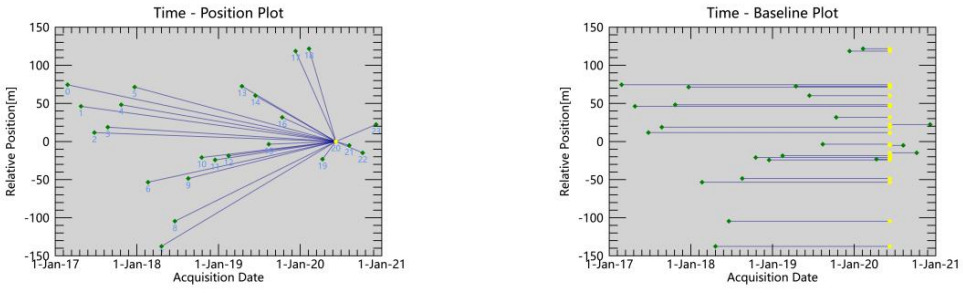

Figure 3. The temporal and spatial baseline distributions of the SAR interferograms from the Sentinel-1

4. RESULT

As shown in Figure 4, we generated 24 deformation results. Most areas are green in color. This means that deformation is relatively stable. The western region is relatively more yellow in color compared to the eastern region, which shows that it has slight ground uplift in the west compared to the east. The mean velocity(mm/year) maps of the final geocoded displacements generated from Sentinel-1 data is shown in

Figure 5. The color cycle from blue to red indicates the positive to negative velocities in the satellite line of sight direction. The positive values indicate that the surface is moving the opposite direction of movement(i.e., uplift) while the negative values indicate that the surface is moving away from the satellite(i.e., subsidence). As shown in Figure 5, most areas show a yellow color, a few areas show a blue-cyan color and red. This means that from a general point of view, most areas have slight uplift, a few areas have slight subsidence and part of areas have a more pronounced uplift.

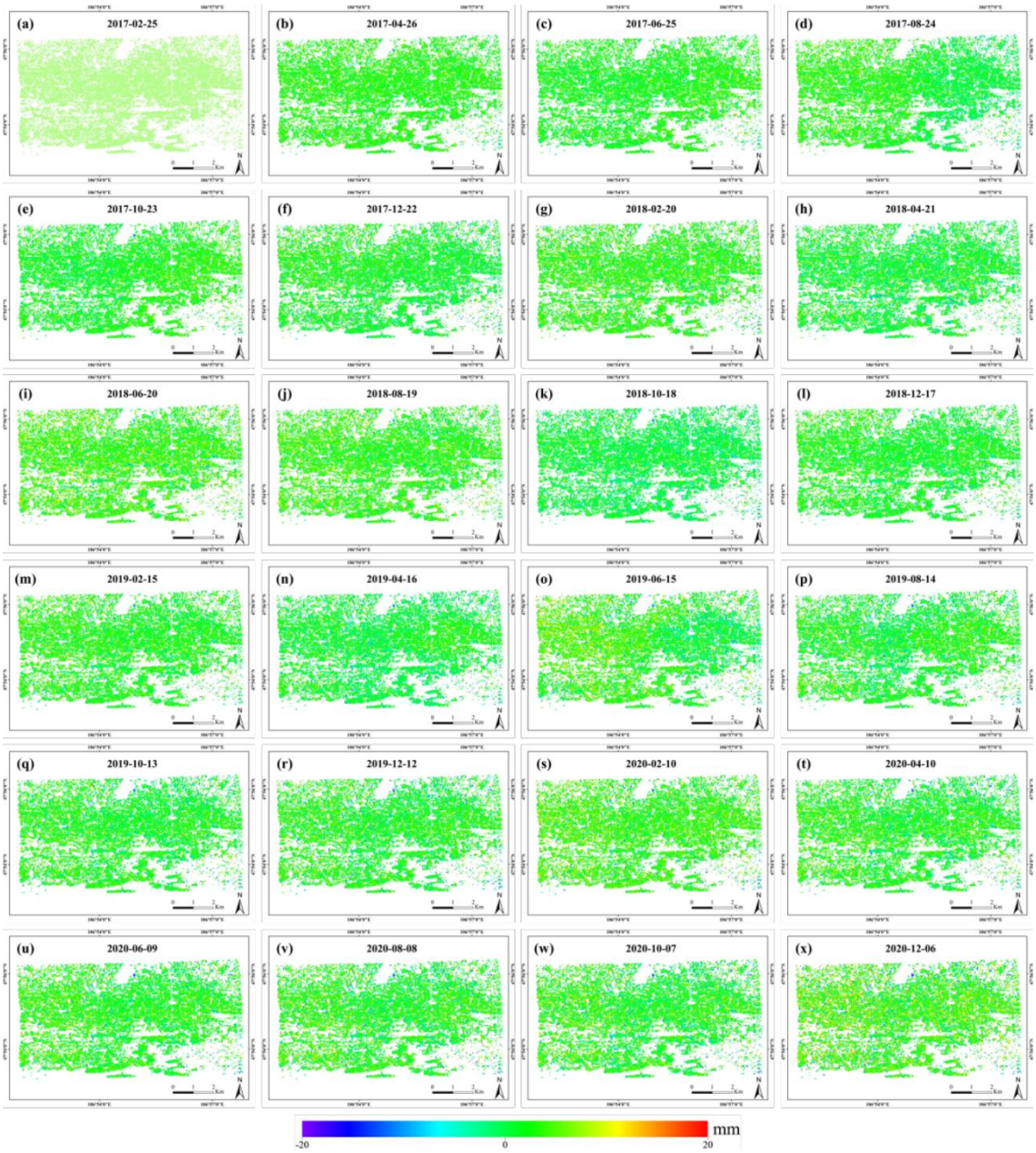

Figure 4 Time-series deformation results

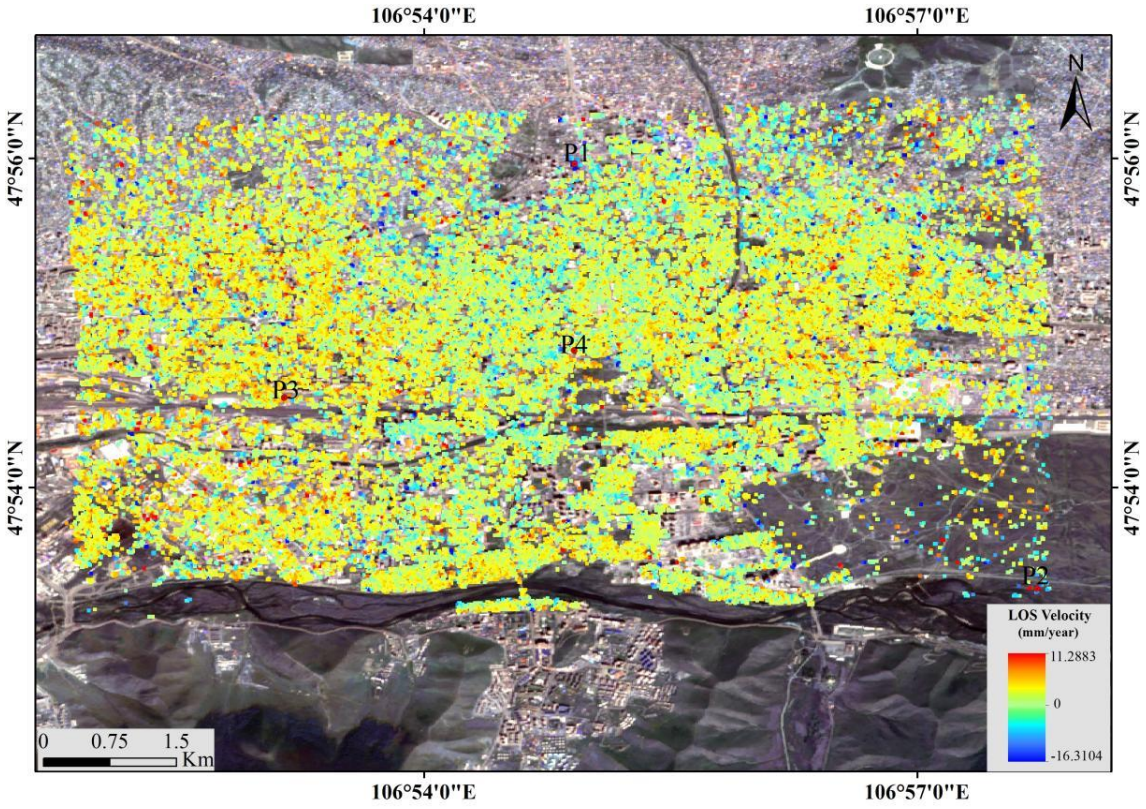

Figure 5. Estimated mean displacement velocity using the PS-InSAR method

The histograms of the estimated displacement velocities by the PS-InSAR method for the study area is shown Figure 6. We can see that most areas are stable and the percentage of areas with significant uplift or subsidence is relatively small. Combined with Figure 5, it is obviously seen that the central part shows a subsidence trend, while the remote areas show uplift. And land subsidence is more obvious near roads and rivers The average displacement rate and the the standard deviation were 0.17 and 1.01 mm/year.

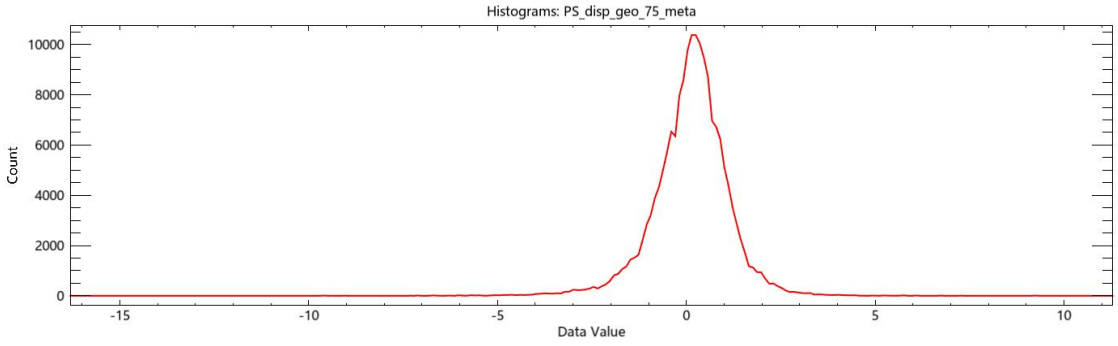

Figure 6. Histogram distribution for the Sentinel-1 derived displacement rates from 2017 to 2020

In the study area, we selected several PS targets, P1-P4, as examples to present the variations during the monitoring period. And the details are list in Table 1. As we can see, among the four points, two points(i.e., P1 and P2) are going on the subsidence, while the other ones(i.e., P3 and P4) are going on the uplifts. From Table 2, the overall deformation is continued lifted and the cumulative lift volume is up to 40.26 mm during the study period. For P1 and P2, the value of the displacement is mostly negative. And for P3 and P4, the value of the displacement is mostly positive. Combined with Figure 7, we can clearly see that overall deformation curve is relatively flat and slowly rising. The displacement curves of P1 and P2 gradually decrease and the magnitude of P1 is greater than that of P2. Similarly the displacement curves of P3 and P4 gradually increase and the magnitude of P4 is greater than that of P3.

Table 1 Four example points of the land deformation from 2017 to 2020

Acquisition Date	All(mm)	P1	P2	P3	P4
2017-02-25	0	0.000000	0.000000	0.000000	0.000000
2017-04-26	2.3166	-9.904840	7.570870	-2.514523	1.588917
2017-06-25	1.7967	-3.908916	10.633374	-4.716097	0.563755
2017-08-24	1.4876	-7.065802	-5.247697	-6.329900	4.670218
2017-10-23	1.696	-13.662559	-11.810861	2.154894	3.063858
2017-12-22	1.2331	-7.932504	-1.896488	0.943090	0.488502
2018-02-20	2.3986	-7.781427	-3.536313	3.362514	7.064333
2018-04-21	0.8249	-9.662992	-3.400131	1.107172	3.794878
2018-06-20	2.9202	-11.059554	-2.732981	2.566521	4.490239
2018-08-19	2.4951	-11.866360	-5.857163	4.421940	7.905241
2018-10-18	0.0575	-13.937333	-10.423137	2.020689	3.978563
2018-12-17	1.4325	-13.412519	-10.008253	-1.839836	10.294251
2019-02-15	1.9087	-13.377087	-6.160975	-1.726647	17.748199
2019-04-16	0.5952	-15.438073	-9.453962	3.439562	7.248229
2019-06-15	2.0751	-15.897415	-7.538808	3.252789	-1.269473
2019-08-14	1.3091	-15.266367	-7.157572	4.442051	6.916849
2019-10-13	1.4827	-17.100227	-8.737642	5.584599	6.192159
2019-12-12	1.5214	-16.533060	-10.432364	2.854703	7.489510
2020-02-10	2.7631	-16.456417	-13.307131	4.707036	8.297917
2020-04-10	1.6368	-20.155151	-9.741889	6.057177	7.759476
2020-06-09	1.8774	-18.824764	-11.315198	6.813284	9.131284
2020-08-08	1.7878	-19.858942	-7.337125	7.878085	9.531871
2020-10-07	1.7094	-17.457981	-14.456767	7.582084	7.827641
2020-12-06	2.9303	-18.455595	-11.730286	15.502795	11.630283

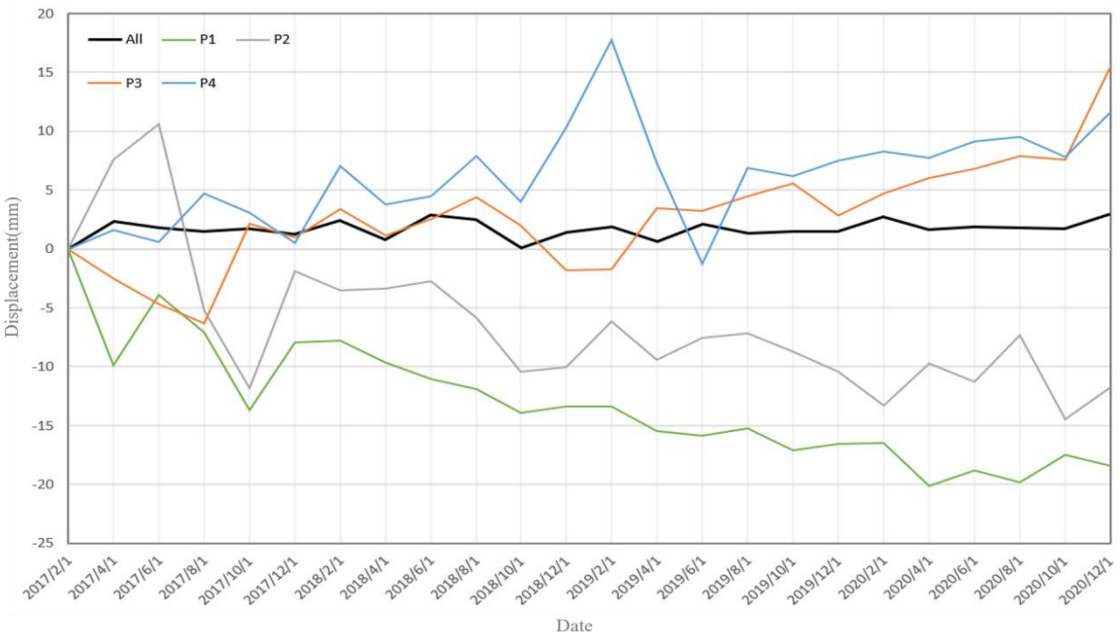

Figure 7. Land deformation curve from 2017 to 2020

5. DISCUSSION

This study attempted to analyse the time-series displacements of Ulaanbaatar by the InSAR method. Firstly, during the processing, we found that the PS-InSAR method is superior to the SBAS-InSAR method because our study area is the urban section of Ulaanbaatar. If the study area is non-urban vegetated areas, the SBAS-InSAR method may be better. Secondly, during the PS-InSAR processing, we found that VV polarisation, compared to the VH polarisation, is superior in terms of PS targets selection.

As shown in Figure 8, we derived a displacement map covering the 3D Live View. Most areas have light lift and some areas have subsidence. For the light uplifts or stability, accounting for a higher percentage, may be caused by the several reasons below. Firstly, viewing the historical images of the study area through Google Earth, it was found that no new housing structures of any kind were built on a large scale in most areas during the study period, which reduced the pressure on the ground to a certain extent. Secondly, by reviewing the information, Ulaanbaatar has become more aware of water conservation in recent years and groundwater extraction is more stable, which makes the ground more stable. Thirdly, it also may be caused by the influence of the surrounded mountains' terrain movement, which could be further explored. While for the subsidence, accounting for a relatively lower percentage, may be caused by the local small-scale construction of new buildings and relatively serious groundwater use in the area.

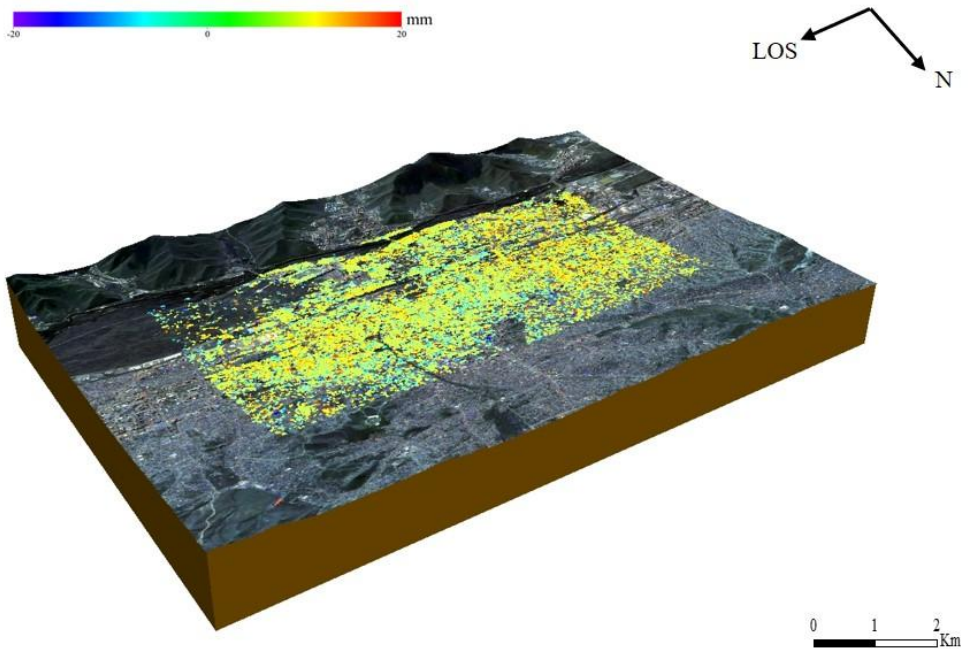

Figure 8 displacement map covering the 3D Live View

6. CONCLUSION

In this paper, to monitor the long-term land deformation in Ulaanbaatar, we propose the application of PS-InSAR with the use of Sentinel-1 data from 25 February 2017 to 6 December 2020. The results that: (1) for the study area, the PS-InSAR method is superior to the SBAS-InSAR method. (2) Most areas have light uplift and some areas have subsidence. The average displacement rate and the the standard deviation were 0.17 and 1.01 mm/year. And the land deformation is in a stable condition overall during the recent years. (3) The ground deformation is mainly stable in the central area of the city, while the light uplift is mainly in the edge. And land subsidence is more obvious near roads and rivers. In this paper, land subsidence in the study area was monitored and the inverted results were obtained. However, the shortcoming is that the results

were not compared and analyzed with relevant data, and thus the causes of uplift or subsidence were not explored more deeply. Therefore, in the subsequent study, the inverse ground deformation results will be correlated with groundwater level data, geological data, and building density data to further explore the main causes of ground deformation occurring in Ulaanbaatar.

REFERENCE

Pradhan, B., et al., 2014. Land subsidence susceptibility mapping at Kinta Valley (Malaysia) using the evidential belief function model in GIS. Natural Hazards, 73(2), pp. 1019-1042.

Raspini, F. , et al., 2014. Ground subsidence phenomena in the Delta municipality region (Northern Greece): Geotechnical modeling and validation with Persistent Scatterer Interferometry. International Journal of Applied Earth Observation & Geoinformation, 28, pp. 78-89.

Oruji, S., et al., 2022. Evaluation of Land Subsidence Hazard on Steel Natural Gas Pipelines in California. ScienceDirect.

Jian, W ., et al., 2011. Coal mining GPS subsidence monitoring technology and its application. Mining Science and Technology (China). 21(004), pp. 463-467.

Amelung, F., et al., 1999. Sensing the ups and downs of las vegas: insar reveals structural control of land subsidence and aquifer-system deformation. Geology, 27(6), pp. 483-486.

Cianflflone, G., et al., 1999. InSAR time series analysis of natural and anthropogenic coastal plain subsidence: The case of sibari (Southern Italy). Remote Sensing.

Fikri, S., et al., 2021. Application of Different Coherence Threshold on PS-InSAR Technique for Monitoring Deformation on the LUSI Affected Area During 2017 and 2019. IOP Conference Series: Earth and Environmental Science.

Aguiar, P., et al., 2021. Multivariate Outlier Detection in Postprocessing of Multi-temporal PS-InSAR Results using Deep Learning. Procedia Computer Science, 181(5), pp. 1146-1153.

Lyu, M., et al., 2020. Detection of Seasonal Deformation of Highway Overpasses Using the PS-InSAR Technique: A Case Study in Beijing Urban Area. Remote Sensing, 12(18), pp. 3071.

Zhang, X., et al., 2022. Inversion of Groundwater Storage Variations Considering Lag Effect in Beijing Plain, from RadarSat-2 with SBAS-InSAR Technology. Remote Sensing, 14, pp. 991.

Mingze,Y., et al., 2021. Subsidence Monitoring Base on SBAS-InSAR and Slope Stability Analysis Method for Damage Analysis in Mountainous Mining Subsidence Regions. Remote Sensing, 13(16), pp. 3107.

Milillo, P., et al., 2019. Pre-collapse space geodetic observations of critical infrastructure: The Morandi Bridge, Genoa, Italy. Remote Sensing, 11(12), pp. 1403-.

Xiong, S., et al., 2021. Time-Series Analysis on Persistent Scatter-Interferometric Synthetic Aperture Radar (PS-InSAR) Derived Displacements of the Hong Kong-Zhuhai-Macao Bridge (HZMB) from Sentinel-1A Observations. Remote Sensing, 13(4), pp. 546.

Hamiduddin, I., et al., 2021. Social Sustainability and Ulaanbaatar's 'Ger Districts': Access and Mobility Issues and Opportunities. Sustainability, 13(20), pp. 1-16.

Yusupujiang, A., et al., 2018. Multi-Sensor InSAR Analysis of Progressive Land Subsidence over the Coastal City of Urayasu, Japan. Remote Sensing, 2018, 10(8), PP. 1304-.